ADVANCED FUNCTIONAL MATERIALS

Supporting Information

for *Adv. Funct. Mater.,* DOI: 10.1002/adfm.202103477

A Broad-Spectrum Antimicrobial and Antiviral Membrane Inactivates SARS-CoV-2 in Minutes

*Qingsheng Liu, Yidan Zhang, Wanjun Liu, Long-Hai Wang, Young W. Choi, Megan Fulton, Stephanie Fuchs, Kaavian Shariati, Mingyu Qiao, Victorien Bernat, and Minglin Ma**

Supplementary Information

A broad-spectrum antimicrobial and antiviral membrane inactivates SARS-CoV-2 in minutes

Authors: Qingsheng Liu[1]†, Yidan Zhang[2, 3]†, Wanjun Liu[1], Long-Hai Wang[1], Young W. Choi[4], Megan Fulton[4], Stephanie Fuchs[1], Kaavian Shariati[1], Mingyu Qiao[3], Victorien Bernat[5], Minglin Ma[1,*]

*To whom correspondence should be addressed. Email: mm826@cornell.edu.
† These authors contributed equally to this work.

This file includes:

Figure S1 to S22

Table S1 to S2

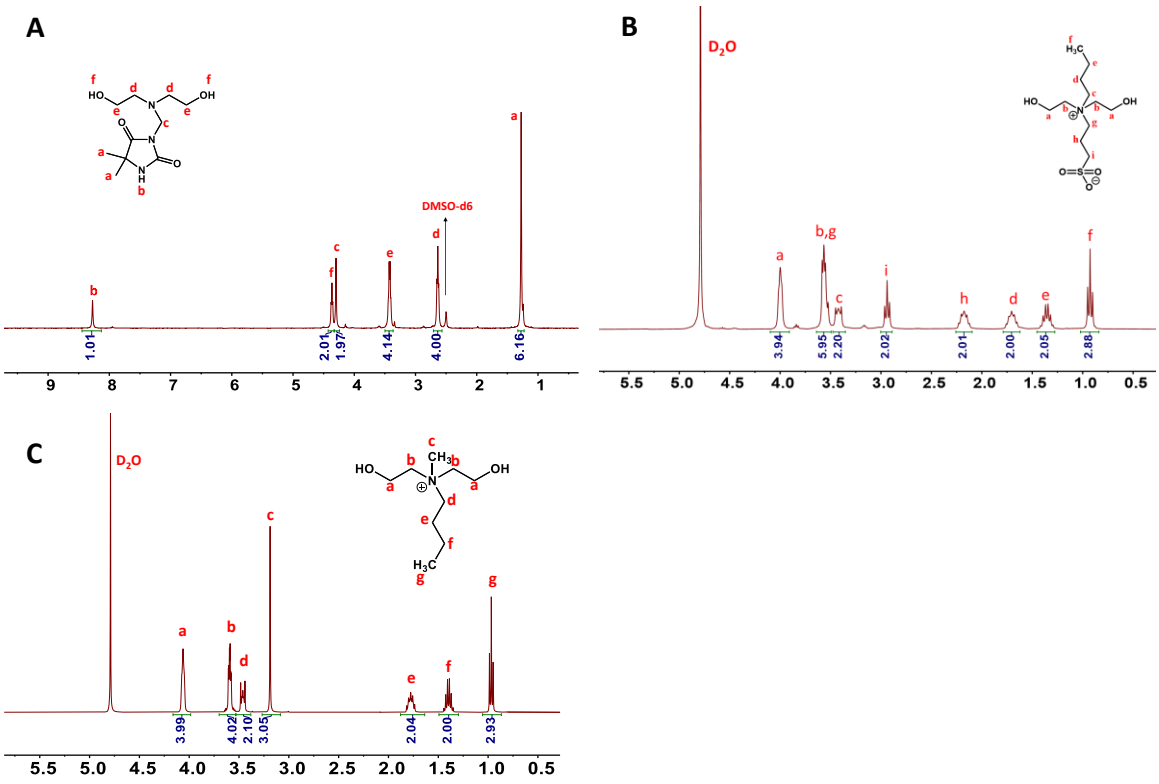

Figure S1. ^{1}H NMR spectrum of (**A**) hydantoin-diol, (**B**) SB-diol, and (**C**) N^{+}-diol monomers at 400 MHz.

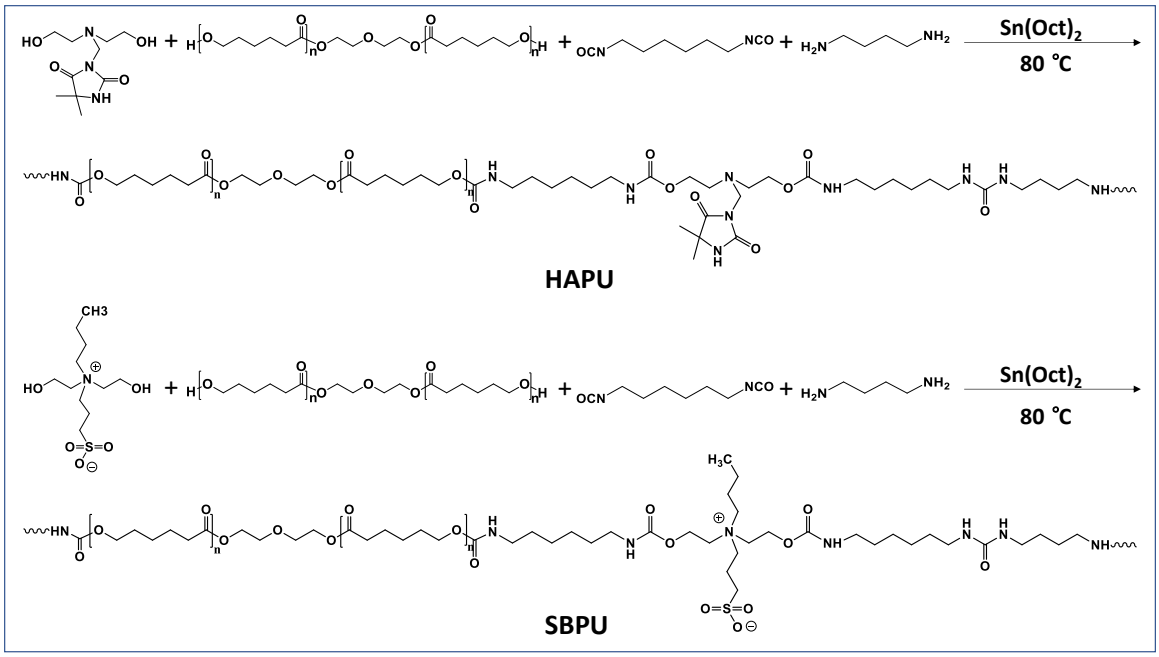

Figure S2. Reaction routes for synthesis of HAPU and SBPU polymers.

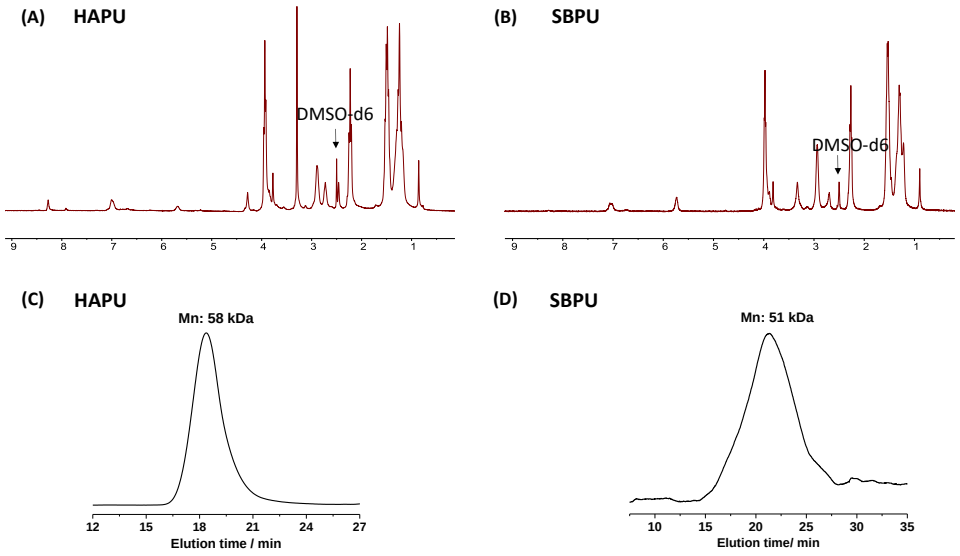

Figure S3. Characterization of HAPU and SBPU polymers. ^{1}H NMR spectrum of (A) HAPU and (B) SBPU polymers; GPC analysis of (C) HAPU polymer (polydispersity: 2.0) in THF solvent and (D) SBPU polymer (polydispersity: 2.9) in DMF solvent.

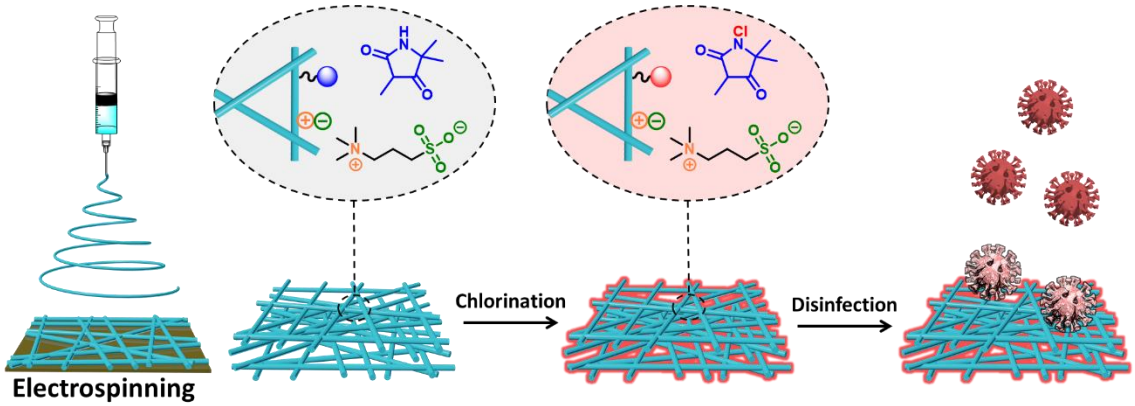

Figure S4. Schematic illustration for the design and fabrication of the anti-viral membrane (AVM).

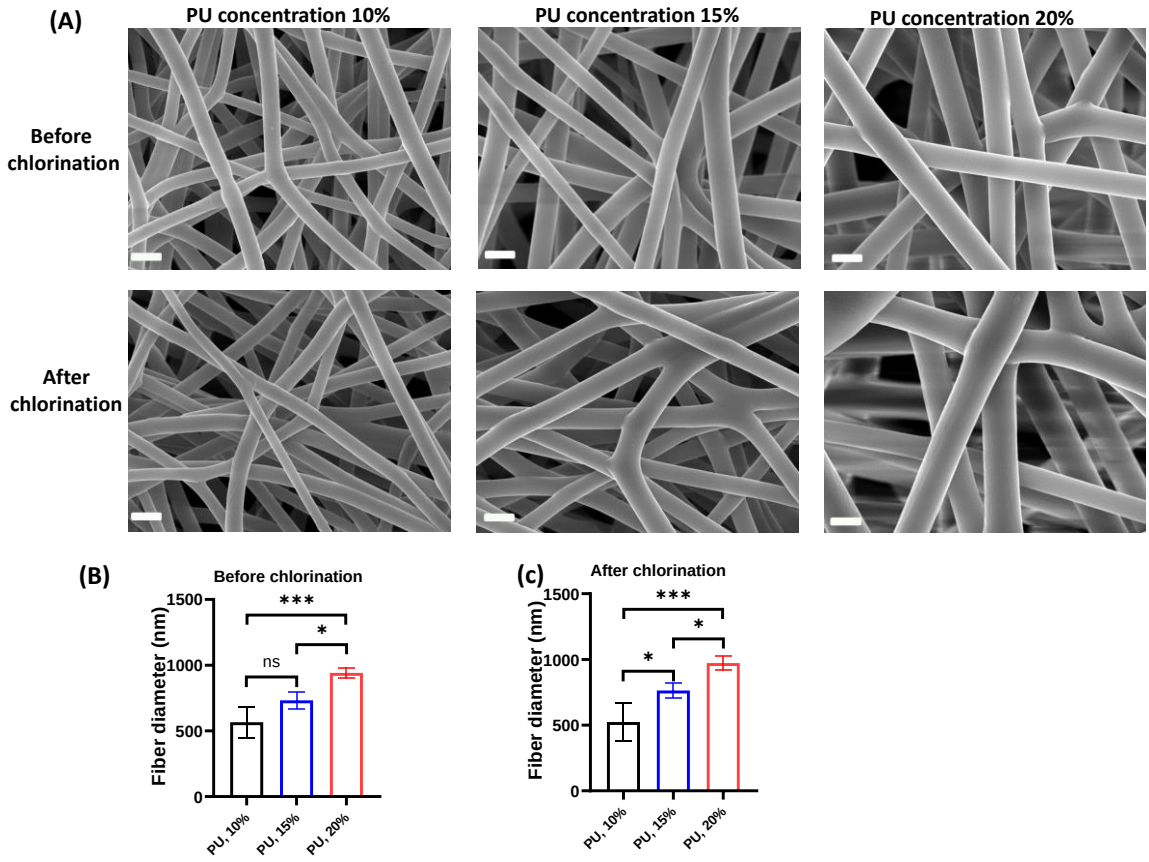

Figure S5. Sub-micron fibrous membranes made of HAPU and SBPU blends: different fiber sizes as a function of total polyurethane (PU) concentration. (**A**) SEM images of the membranes (before and after chlorination) made from different PU concentrations (from left to right: 10% (w/v or g/ml), 15%, and 20%). Scale bar, 1 µm. (**B**) Fiber size of the membranes as a function of PU concentration before chlorination. (**C**) Fiber size of the membranes as a function of PU concentration after chlorination. Mean ± SEM; $n = 6$. ns: not significant, **p*-value <0.05, ****p*-value <0.001

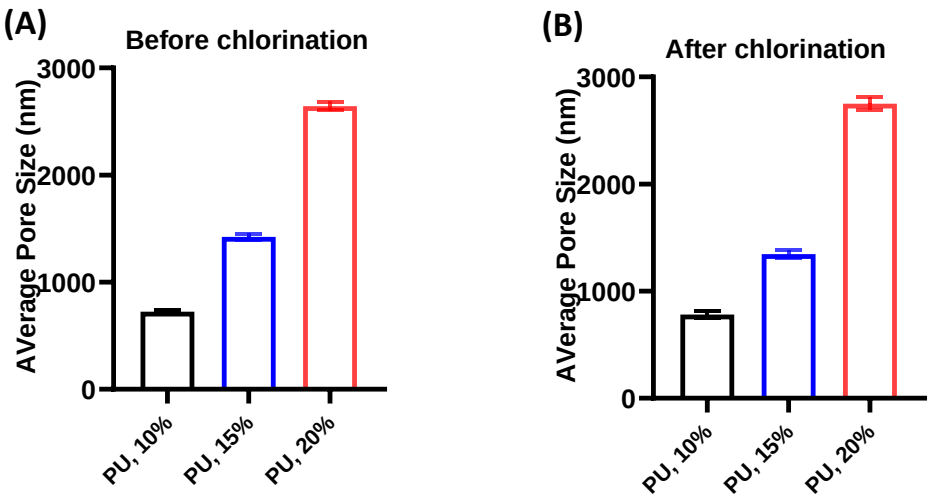

Figure S6. Average pore sizes as a function of total polyurethane (PU) concentration. (**A**) Pore size distribution of the membrane before chlorination. (**B**) Pore size distribution of the membrane after chlorination. Mean ± SEM; $n = 3$.

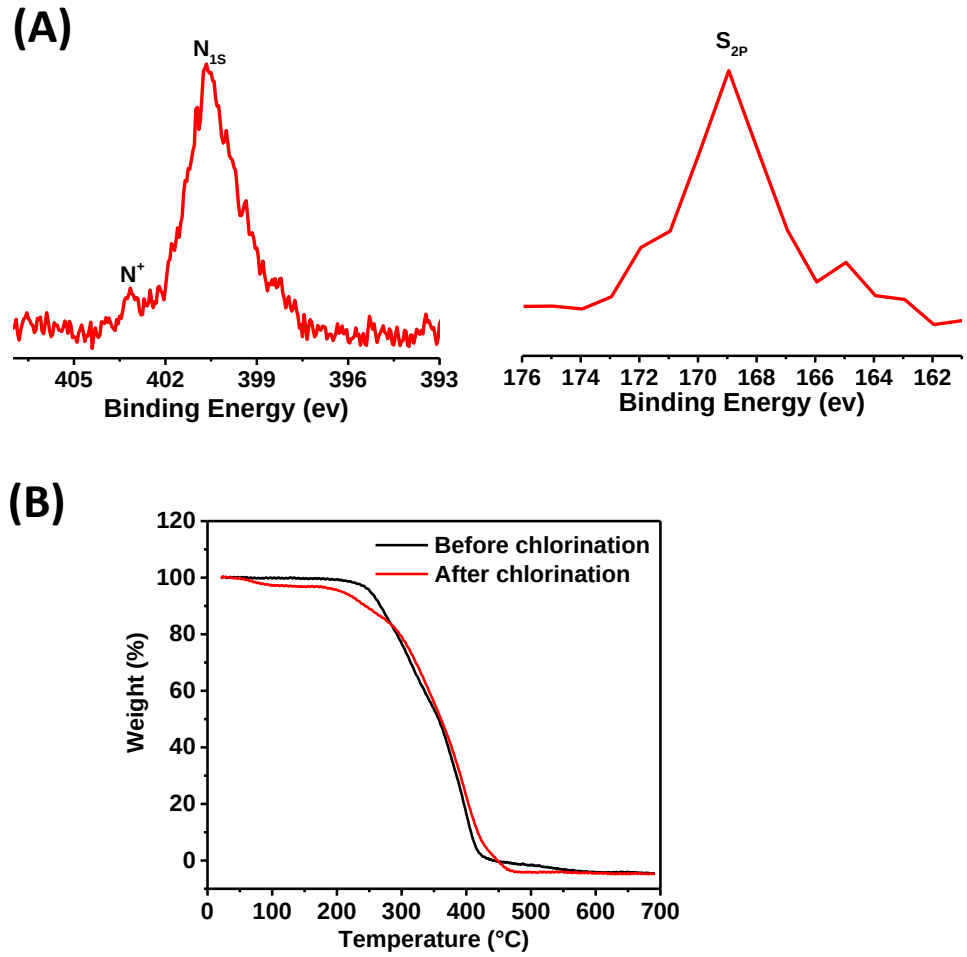

Figure S7. Material characterizations of AVM. (**A**) XPS N_{1s} and S_{2p} spectra of AVM. (**B**) Thermogravimetric analysis (TGA) profile of the membranes before and after chlorination.

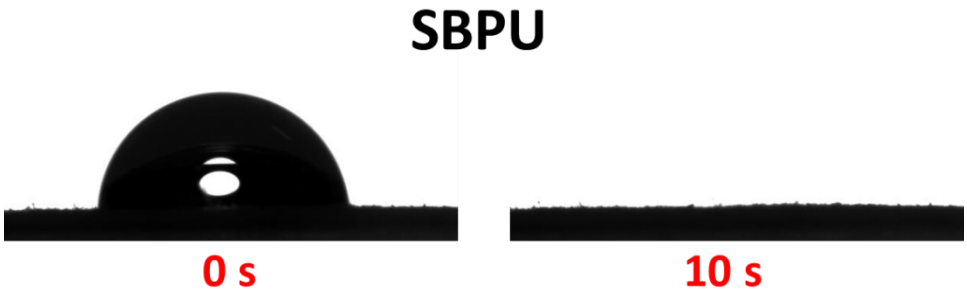

Figure S8. Digital photographs of water droplets on SBPU membranes.

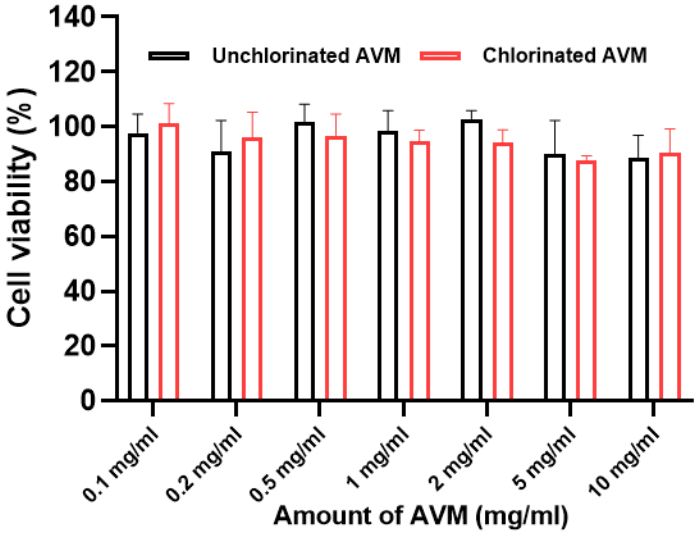

Figure S9. Cytotoxicity of unchlorinated and chlorinated AVM against NIH/3T3 fibroblasts determined by the MTT assay. Data are normalized to the negative control (i.e. cells cultured in the medium only) and expressed as Mean ± SEM (n = 6).

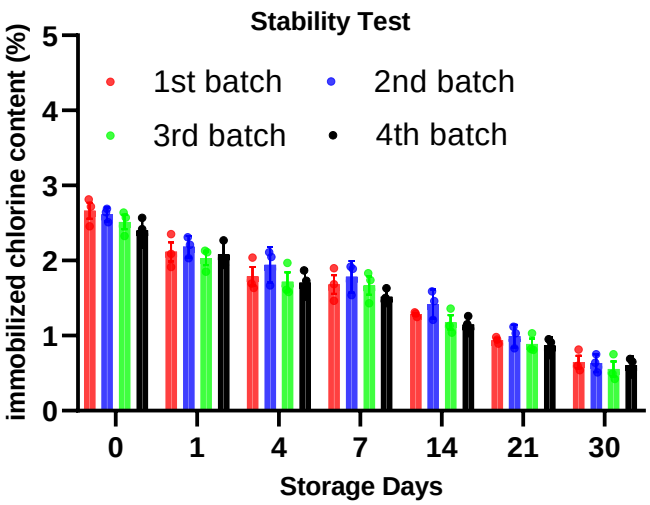

Figure S10. Stability of immobilized chlorine (weight percentage) on AVM made from various batches of polyurethanes under dry condition. Mean ± SEM; $n = 3$.

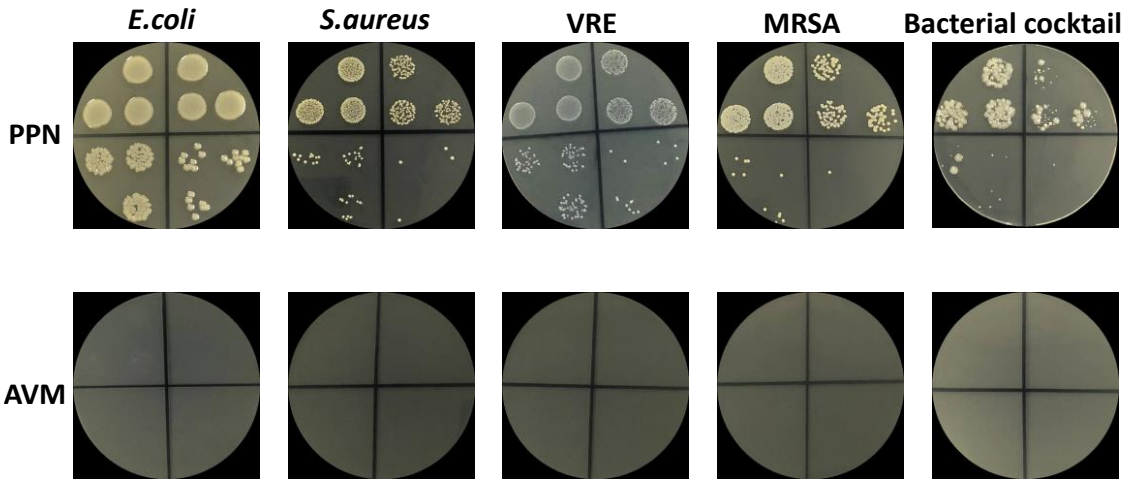

Figure S11. Photographs from bacterial culture plates with different bacterial strains after a 1 min exposure to PPN membrane and AVM.

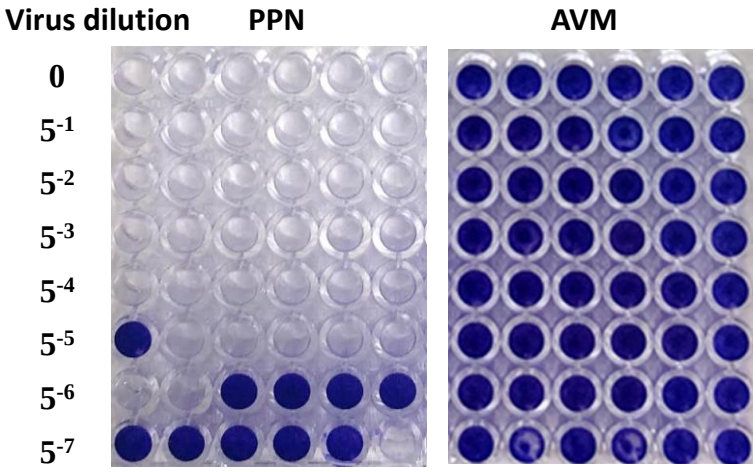

Figure S12. Crystal violet stained $TCID_{50}$ plates of AVM and PPN membrane against FCV after 2h contact. Crandell-Rees Feline Kidney (CRFK) cells were infected with FCV and stained with crystal violet for detection of CPE after 7-day incubation.

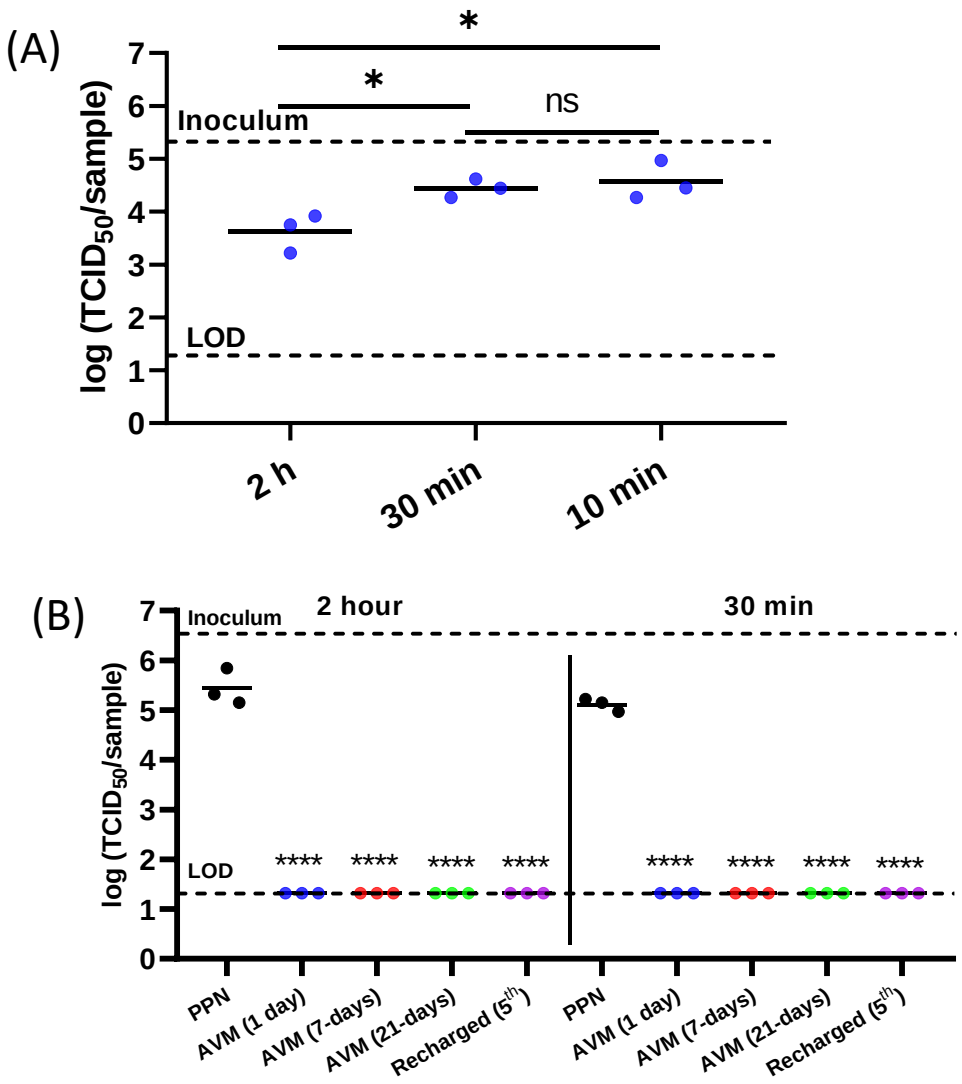

Figure S13. The viability of FCV on various membranes. (**A**) Viable titer of FCV on the membrane made of HAPU and SBPU before chlorination. (**B**) Viable titer of FCV on the AVM with different shelf times or recharged, after 30 min or 2 h contact. PPN membranes were used as a control. Mean ± SEM; n = 3. ns: not significant; **p*-value <0.05; *****p*-value <0.0001.

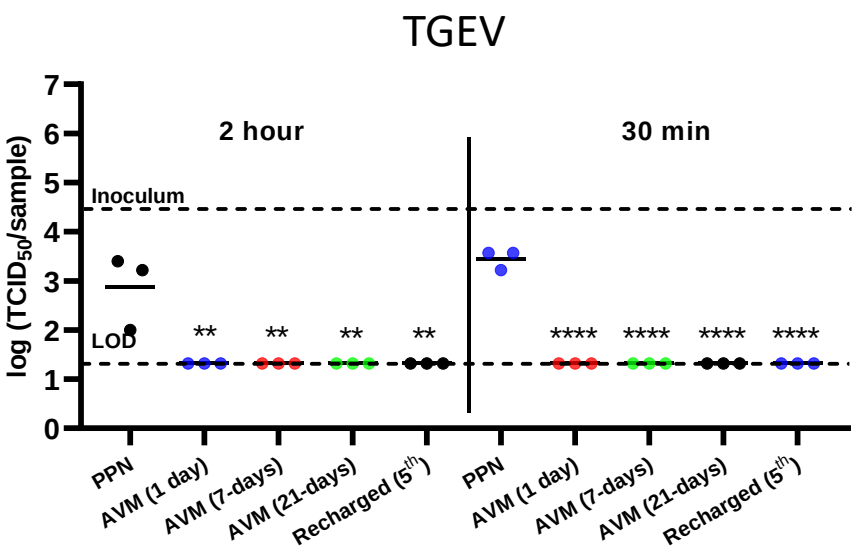

Figure S14. Viable titer of TGEV on the AVM with different shelf times or recharged, after 30 min or 2 h contact. PPN membranes were used as a control. n = 3 for each group. ***p*-value <0.01; *****p*-value <0.0001.

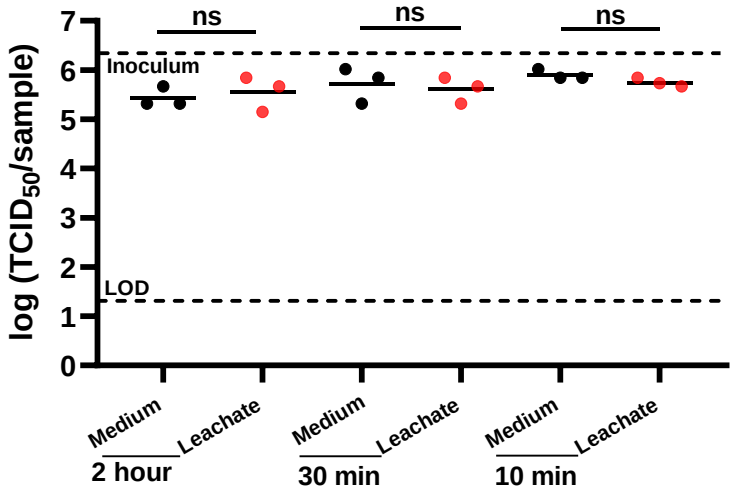

Figure S15. Effect of leachate from AVM on FCV viability after 10 min, 30 min or 2 h of contact. n = 3 for each group. ns: not significant.

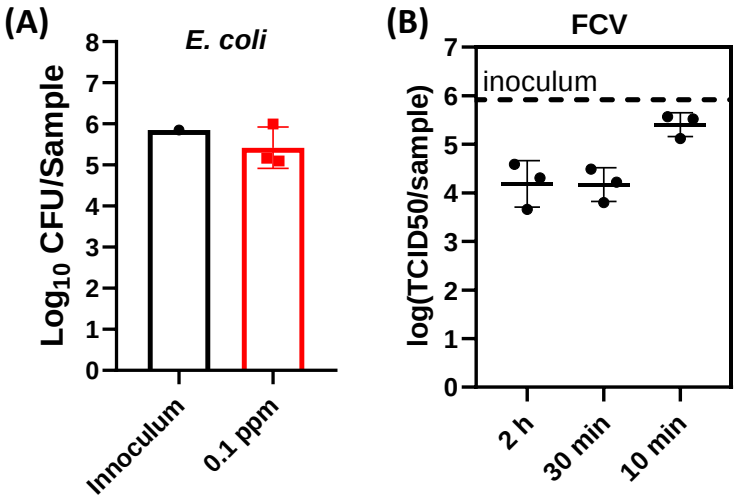

Figure S16. The (a) antimicrobial and (b) antiviral activities of diluted commercial bleach containing 0.1 ppm chlorine. n = 3 for each group.

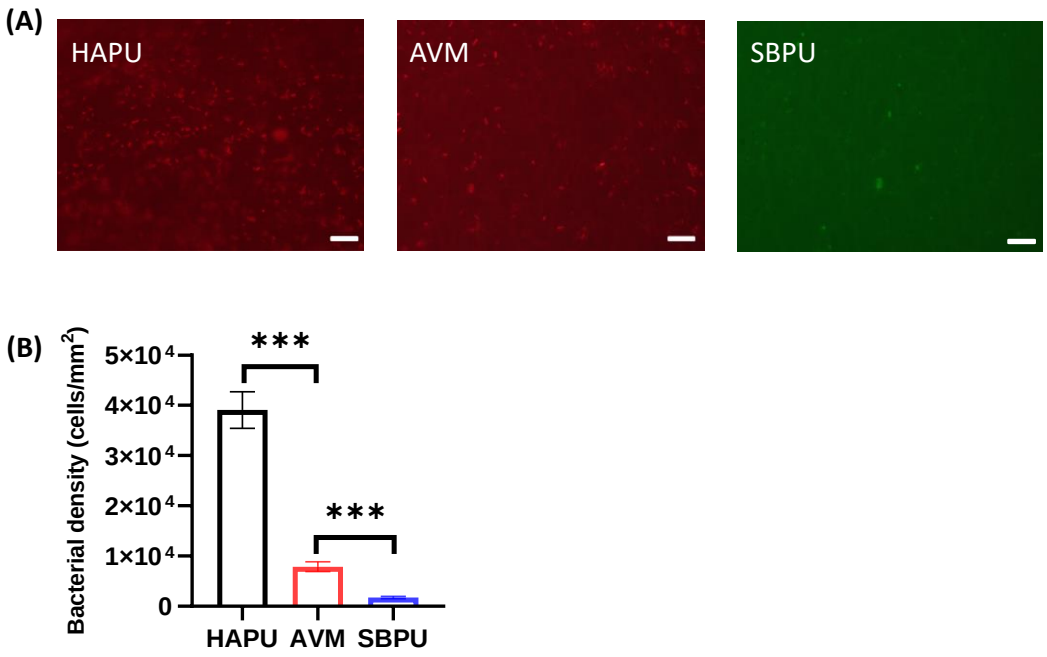

Figure S17. Bacterial attachment on the various membranes. (**A**) Representative fluorescence microscopy images of *E. coli* attached on different membranes, and (**B**) corresponding bacterial density accumulated on the membranes. Bar = 10 μm. Mean ± SEM; $n = 3$. ***p-value <0.001.

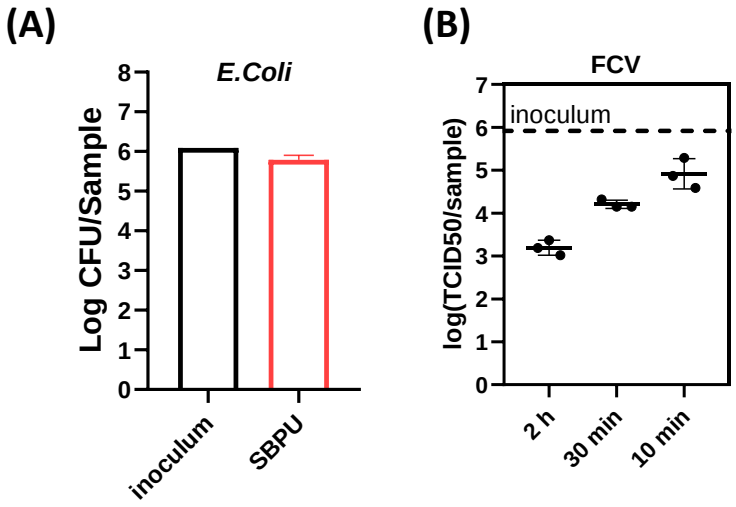

Figure S18. The (a) antimicrobial and (b) antiviral activities of unchlorinated SBPU membrane. n = 3 for each group.

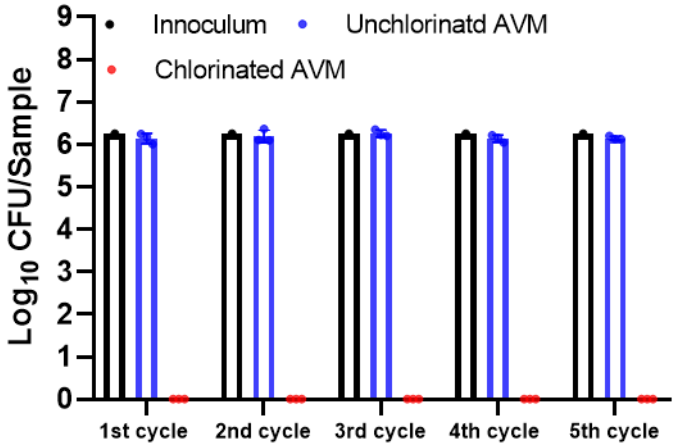

Figure S19. Antibacterial activity of AVM with single chlorination after repeated challenges. Mean ± SEM; n = 3.

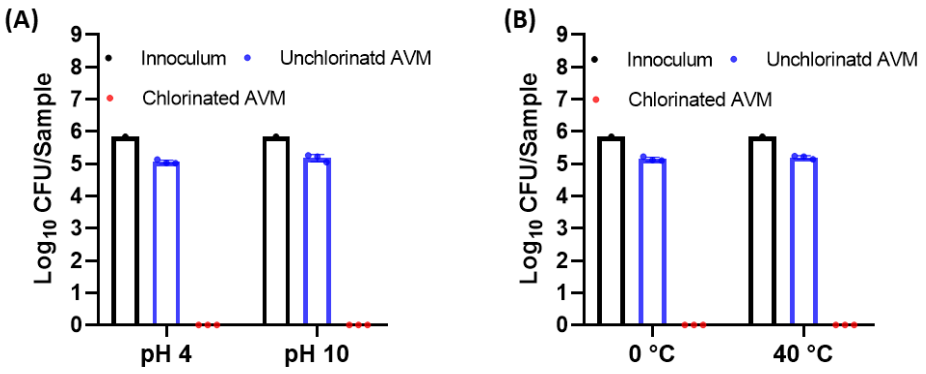

Figure S20. Bactericidal efficacies of AVM against *E. coli* in different (A) pH conditions after 1 day of incubation and (B) temperature conditions for 3 days of incubation. Mean ± SEM; n = 3.

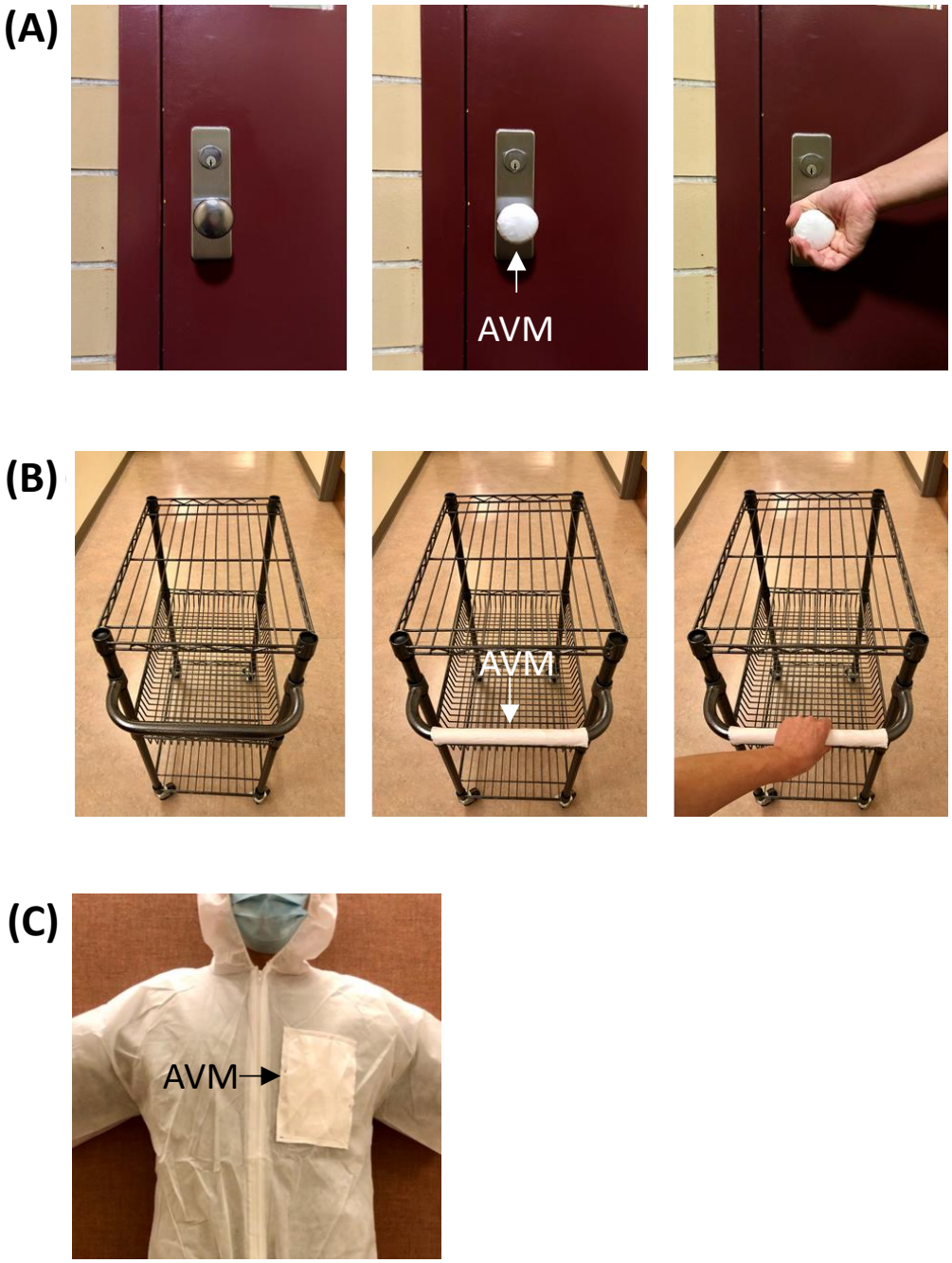

Figure S21. Digital photographs of (**A**) doorknob, (**B**) shopping cart handle and (**C**) protective suit coated with the AVM.

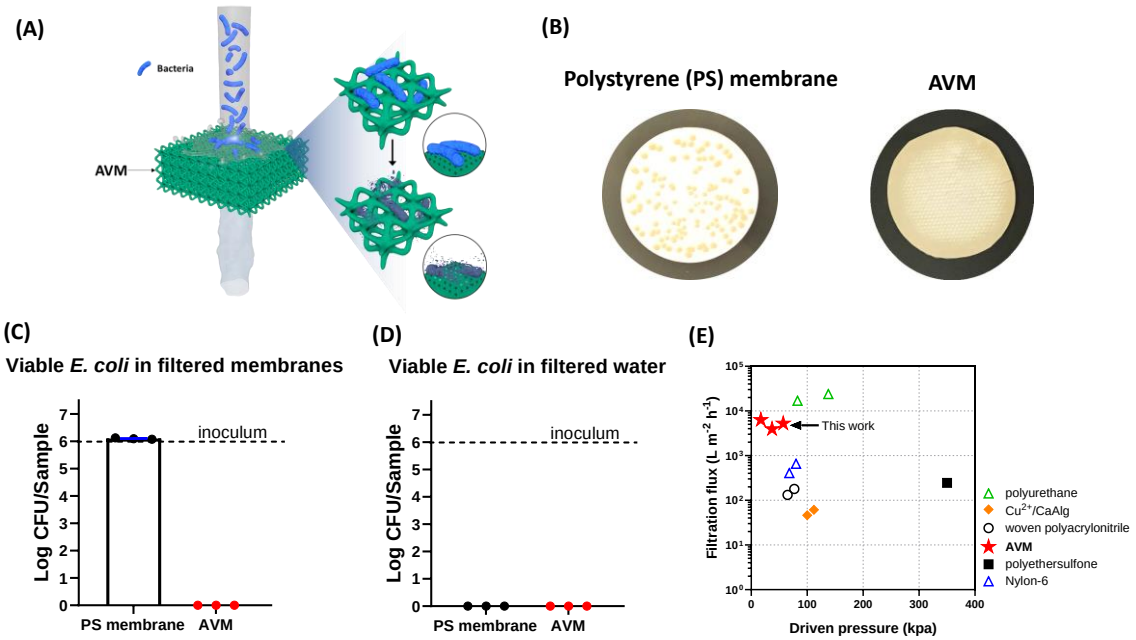

Figure S22. Wastewater filtration application of AVM. (**A**) Schematic demonstration of wastewater filtration process on AVM. (**B**) The culture plates of AVM and control polystyrene filter membrane after disinfecting *E. coli*-containing wastewater. (**C**) Viable *E. coli* recovered from AVM and control polystyrene filter membrane after disinfecting *E. coli*-containing wastewater. No viable E. coli was detected on AVM membrane whereas more than 6 log CFU/sample was detected on analytical polystyrene control filter membrane. (**D**) Viable *E. coli* recovered from the filtered water. (**E**) Comparison of filtration flux of AVM and previously reported filtration materials. The hydrophilic AVM not only effectively disinfected the microbe-contaminated water, but also showed relatively high filtration flux with a relatively low driven pressure compared to previously reported materials including hydrophobic and hydrophilic membranes.[1]

Table S1. Strains in cocktail of 14 clinically isolated pathogen strains from soldiers in field hospitals.

No.	Strain	Source
1	*Pseudomonas. aeruginosa*	Blood
2	*Pseudomonas. aeruginosa*	Tissue
3	*Enterobacter. cloacae*	Urine
4	*Enterobacter. cloacae*	Urine
5	*Acinetobacter. baumannii*	Surveillance
6	*Acinetobacter. baumannii*	Respirator
7	*Klebsiella. pneumoniae*	Urine
8	*Klebsiella. pneumoniae*	Respirator
9	*Staphylococcus. aureus*	Surveillance
10	*Staphylococcus spp.*, coagulase negative	Fluid
11	*Enterococcus. faecium*	Abscess
12	*Enterococcus. faecium*	Wound
13	*Streptococcus. pyogenes*	Blood
14	*Streptococcus. pyogenes*	Blood

Note: The above strains were received from Walter Reed Army Institute of Research & Naval Medical Research Center.

Table S2. Bactericidal efficacies of AVM and PPN (control) against various bacteria in 15 or 30 min.

Sample	Contact time	Recovered bacteria (mean log [CFU/sample])				
		E. coli	***S. aureus***	**VRE**	**MRSA**	**Bacterial cocktail**
PPN	30 min	4.90	4.74	6.04	4.50	4.75
AVM	30 min	0	0	0	0	0
PPN	15 min	5.40	5.24	6.12	5.24	5.40
AVM	15 min	0	0	0	0	0

References

[1] a) D. Aussawasathien, C. Teerawattananon, A. Vongachariya, *Journal of membrane science* **2008**, 315, 11; b) N. Maximous, G. Nakhla, W. Wan, *Journal of membrane Science* **2009**, 339, 93; c) H. R. Pant, H. J. Kim, M. K. Joshi, B. Pant, C. H. Park, J. I. Kim, K. Hui, C. S. Kim, *Journal of hazardous materials* **2014**, 264, 25; d) T. Bai, K. Zhao, Z. Lu, X. Liu, Z. Lin, M. Cheng, Z. Li, D. Zhu, L. Zhang, *Chinese Chemical Letters* **2021,** 32, 1051; e) F. Zhao, S. Chen, Q. Hu, G. Xue, Q. Ni, Q. Jiang, Y. Qiu, *Separation and Purification Technology* **2017**, 175, 130.